Predictive Systems Biology Modeling: Unraveling Host Metabolic Disruptions and Potential Drug Targets in Acute Viral Infections

Gong-Hua Li[1,5#,*], Feifei Han[2#], Rong-Hua Luo[3,4#], Peng Li[2], Chia-Jung Chang[2], Weihong Xu[2], Xin-Yan Long[3,4], Jing-Fei Huang[1], Yong-Tang Zheng[3,4*], Qing-Peng Kong[1,5*], Wenzhong Xiao[2*]

[1] State Key Laboratory of Genetic Resources and Evolution, Key Laboratory of Healthy Aging Research of Yunnan Province, Kunming Key Laboratory of Healthy Aging Study, KIZ/CUHK Joint Laboratory of Bioresources and Molecular Research in Common Diseases, Kunming Institute of Zoology, Chinese Academy of Sciences, Kunming, Yunnan 650201, China;
[2] Immune and Metabolic Computational Center, Massachusetts General Hospital, Harvard Medical School, Boston, MA 02114, USA;
[3] Key Laboratory of Animal Models and Human Disease Mechanisms of the Chinese Academy of Sciences, KIZ-CUHK Joint Laboratory of Bioresources and Molecular Research in Common Diseases, Kunming Institute of Zoology, Chinese Academy of Sciences, Kunming, Yunnan 650223, China;
[4] Kunming National High-level Biosafety Research Center for Non-human Primates, Center for Biosafety Mega-Science, Kunming Institute of Zoology Chinese Academic of Sciences, Kunming, Yunnan 650107, China;
[5] CAS Center for Excellence in Animal Evolution and Genetics, Chinese Academy of Sciences, Kunming 650223, China.

[#]These authors contributed equally.

*Correspondence: Wenzhong Xiao (wenzhong.xiao@mgh.harvard.edu), Qing-Peng Kong(kongqp@mail.kiz.ac.cn), Yong-Tang Zheng(zhengyt@mail.kiz.ac.cn) or Gong-Hua Li (ligonghua@mail.kiz.ac.cn).

Abstract

Background: Host response is critical to the onset, progression, and outcome of viral infections. Since viruses hijack the host cellular metabolism for their replications, we hypothesized that restoring host cell metabolism can efficiently reduce viral production.

Results: Here, we present a viral-host Metabolic Modeling (vhMM) method to systematically evaluate the disturbances in host metabolism in viral infection and computationally identify targets for modulation by integrating genome-wide precision metabolic modeling and cheminformatics. We applied vhMM to SARS-CoV-2 infections and identified consistent changes in host metabolism and gene and endogenous metabolite targets between the original SARS-COV-2 and different variants (Alpha, Delta, and Omicron). Among six compounds predicted for repurposing, *methotrexate*, *cinnamaldehyde*, and *deferiprone* were tested *in vitro* and effective in inhibiting viral production with IC50 less than 4uM. Further, an analysis of real-

world patient data showed that cinnamon usage significantly reduced the SARS-CoV-2 infection rate with an odds ratio of 0.65 [95%CI: 0.55~0.75].

Conclusions: These results demonstrated that vhMM is an efficient method for predicting targets and drugs for viral infections.

Keywords: vhMM, viral diseases, SARS-COV-2, host metabolism, drug repurposing, methotrexate, cinnamaldehyde, deferiprone

Background

Viral infections have consistently been a significant health concern throughout human society [1, 2]. Despite intensive research, a few drugs are FDA-approved to date for viral diseases[3-5]. The emergence of viral variants has also significantly impacted the efficacy of available therapeutics and vaccines[6-9]. There is still a critical need for developing new agents to treat viral infectious diseases. While current small-molecule drugs target viral proteins, investigations into the host pathways provide opportunities for discovering new therapeutic agents with different mechanisms that are either efficacious alone or in combination therapy. Since viruses hijack host cellular metabolism for replications, which require high energy expenditure and a large number of host metabolites[10] for the production of viral components, such as proteins, RNA, and lipids, we hypothesize that restoring host cell metabolism can efficiently negate viral production.

Genome-scale metabolic modeling can capture metabolic states of cells or tissues[11] and has been applied to understanding the mechanisms of diseases, such as obesity[12], NAFLD [13], cancer[14], and Alzheimer's disease[15]. It has also been utilized to study human cell metabolic changes after viral infection and infer gene targets[16-18]. However, how to directly predict candidate drugs for viral infections by targeting the host metabolic response remains challenging.

We recently developed an algorithm of precision metabolic modeling (GPMM) by quantitative integration of the enzyme kinetics information from knowledge bases and enzyme levels from transcriptome and proteome data[19]. Together with the *in silico* genome-wide gene and metabolite knock-in/knock-out capability[20], this approach allows systematic evaluations of genes and endogenous metabolites as candidate targets to modulate the host metabolism. In addition, recent developments in chemoinformatics have enabled computational drug discovery by comprehensive comparison of molecular structures[21, 22] and integrated bioactivity data between a large number of small molecule compounds and the candidate targets[23].

Here we integrate these algorithms to unravel the host metabolic disruptions in viral infection and discover potential antiviral targets. We applied this method to analyze the genomic data of human cells infected by SARS-CoV-2 and identified gene and metabolite targets as well as drug candidates that inhibit both the original virus and its variants. We performed *in vitro* validation experiments on three out of six predicted drug candidates and found that they can effectively inhibit viral production in cell lines. Further, an analysis of real-world data from five major hospitals showed that cinnamon usage significantly reduced the risk of COVID-19 infection. Taken together, this computational approach is effective in aiding the modulation of host metabolism against viral infection.

Results

viral-host Metabolic Modeling (vhMM) for modulating host metabolism against viral infection

vhMM was developed to predict drug candidates to modulate host metabolism against viral infection by integrating several procedures, including system-level precision metabolic modeling, *in silico* system-wide knock-out analysis of genes and metabolites on metabolic fluxes, and chemoinformatics to identify drugs targeting these genes and metabolites for repurposing.

As shown in **Figure 1**, a metabolism network model of human cells after viral infection was first constructed that integrated human reconstructed metabolic models (e.g. Recon3D) and the COVID-19 disease map[24]. In total 28 SARS-CoV-2-specific proteins, negative and positive RNAs, and lipids were included in the curated virus-host metabolism map, along with the viral biomass reaction using protein and RNA compositions from the literature[24, 25].

Second, Genome-wide Precision Metabolic Modeling (GPMM), a method we recently developed to quantitatively integrate enzyme kinetics information from curated knowledge bases and enzyme levels from transcriptome and proteome data into metabolic models[19], was applied to characterize changes in metabolic fluxes due to the viral infection by comparing transcriptome data before and after SARS-CoV-2 infection in three cell lines, A549, Calu3 and NHBE[26].

Third, in silico knockout analysis was systematically performed on all the genes and metabolites involved in the model to examine which genes and metabolites can reverse the altered metabolic fluxes in infected cells, using a computationally efficient algorithm FastMM[27]. Since the virus is critically dependent on redirecting many host metabolic pathways for its reproduction in the infected host cells, different from previous studies that only considered the viral biomass reaction, we considered all the metabolic fluxes changed by the infection to predict potential interventions to restore the compromised host metabolism toward homeostasis. This all-against-all knockout analysis gave rise to effect-size matrices of genes and metabolites on metabolic fluxes from which the top genes and endogenous metabolites were identified as potential targets.

Finally, we adapted Chemical Checker (CC)[23], a database of biological and chemical signatures of ~800,000 small molecules, and DrugBank[28], an online database containing information on drugs and drug targets, to predict candidate drugs that mimic the molecular characteristics of the gene and metabolite targets. If two compounds have similar metabolic networks or signaling pathways, we define them as having similar effects if they have the same pharmacological effect; otherwise, they are defined as having opposite effects (Details in **Materials and Methods**).

Evaluation of the host metabolism hijacked by SARS-CoV-2 in infected cells

We analyzed the altered metabolic state of the host cells infected by SARS-CoV-2 using a transcriptome dataset of three viral-infected cell lines (ACE2-induced A549, Calu3, and NHBE)[26]. First, using the viral biomass reaction as the target function, we simulated from the transcriptome data the viral production of SARS-CoV-2 under each of the 13 conditions across

the three cell lines. As shown in **Figure 2A,** compared with the measured viral load, the algorithm effectively predicted the viral production ($r = 0.75$, $p = 0.003$). Next, we identified individual metabolic fluxes and pathways significantly perturbed in each of the cell lines (false discovery rate < 0.01). Notably, we observed a core set of viral perturbed metabolic pathways changed consistently between the three cell lines after SARS-CoV-2 infection (**Figure 2B**). Strikingly, pathways intimately associated with viral production, such as SARS-CoV-2 protein synthesis, sense RNA synthesis, antisense RNA synthesis, and the overall viral biomass, were all significantly up-regulated, while pathways of oxidative phosphorylation (OP), mitochondria transport, glycolysis/gluconeogenesis, and tyrosine metabolism were down-regulated in the aforementioned three cell lines, presumably as the result of the viral reprioritization of the host metabolism to support the synthesis of viral components. Importantly, these results were corroborated in a most recent study that core mitochondrial genes are down-regulated in nasopharyngeal and autopsy tissues of patients after SARS-Cov-2 infection[29].

In silico gene knockouts toward restoring host metabolism after infection

We performed an all-against-all genome-wide single-gene knockout analysis in the three cell lines and computed changes in metabolic fluxes affected by each gene knockout. These resulted in a matrix of significant gene-flux effects for each cell line that included genes and corresponding metabolic fluxes significantly changed in the cell line (log2 fold changes of the fluxes > 0.5 and $p < 0.05$). To be stringent, we only considered gene knockouts that significantly affecting at least three separate fluxes as potential candidates for targets (Details in **Materials and Methods**). In A549, this matrix comprised 181 genes and 213 fluxes, while 166 genes and 228 fluxes in Calu3 and 171 genes and 154 fluxes in NHBE (**Supplementary Table S1-S3**).

We further defined the genes identified as antagonist targets, where the knocked-outs of these genes inhibited the fluxes up-regulated in the viral infection, and as agonist targets, where the gene knocked-outs further decreased the fluxes down-regulated in the viral infection. We hypothesized that inhibiting the antagonist targets or activating the agonist targets helps restore the infection-altered metabolic fluxes toward homeostasis and thus may reduce viral production. Five antagonist and two agonist targets were identified that were consistent in the three cell lines (A549, Calu3, and NHBE) (**Figure 2C, Supplementary Table S4**). The five antagonist targets were PAICS, GART, ATIC, PPAT, and PFAS, which are all enzymes involved in purine synthesis. Purine synthesis has been widely considered a target for developing antiviral and anticancer drugs[30, 31] and can be potentially targeted against SARS-COV-2 infections. The two agonist targets were TYMS (thymidylate synthetase) and DHFR (dihydrofolate reductase).

We investigated whether these gene targets can directly inhibit the major components of viral production, including viral proteins, RNA, lipids, and the viral biomass reaction. The result showed that knockouts of each of the five antagonists reduced every viral component, including viral proteins, RNA, and lipids, as well as the viral biomass reaction in Calu3 and NHBE cell lines (**Supplementary Table S5)**. For the A549 cell line, knockouts of these antagonist targets inhibited viral proteins and RNA, but not viral lipids and the biomass reaction (**Supplementary Table S5)**. These results indicate that targeting these antagonists could inhibit viral production.

In silico screening of endogenous metabolites to modulate host cells after infection

We next conducted an all-against-all metabolite knockout analysis to obtain the potential endogenous metabolites to modulate. Similar to the gene knockout analysis, we only considered

metabolite knockouts that significantly affected at least three separate fluxes as potential candidates for targets (Details in **Materials and Methods**). 462 metabolites were identified as significantly affecting the metabolic fluxes in A549 infected cell line, while 455 and 400 metabolites were identified as significant in Calu3 and NHBE cell lines, respectively (**Supplementary Table S6-S8**).

These metabolites were also characterized into two categories based on their impact on the metabolic fluxes compared with the corresponding changes by the infection. **Figure 2D** and **Supplementary Table S9** showed the 20 endogenous metabolites identified as consistent in the three cell lines. Two agonist endogenous metabolites included methylenetetrahydrofolate(mlthf), and 2-oxoglutarate (akg), and 18 antagonist metabolites included IMP, GTP, adenylosuccinate (dcamp), seven metabolites related to purine synthesis (25aics, air, 5aizc, gar, fgam, pram, and fpram), and eight amino acids (Gly, Cys, Phe, Asn, Lys, Arg, Met, and Thr). IMP was previously identified as an essential metabolite for viral production, and its synthesis has been targeted in antiviral applications [32].

We further investigated whether targeting these metabolites can also directly inhibit viral production. The results showed that targeting any of the 18 antagonist metabolites can not only inhibit the biosynthesis of all the viral components as well as the viral biomass reaction (**Supplementary Table S10).**

Common drug candidates between the original strain and variants of concern (VOCs)

Numerous variants of SARS-CoV-2 have emerged since the pandemic, and so far, at least VOCs have significantly impacted global public health, therapeutics, and vaccines[33]. Therefore, we evaluated whether our results from the study of an original SARS-CoV-2 isolate (IC19) are replicable in independent studies of the different viral isolates (Alpha, Delta, and Omicron) in a cell line (Calu3)[34, 35].

The core set of metabolic pathways identified in IC19 infected cell lines was similarly perturbed by the VOCs (**Figure 3A**), which included the up-regulated SARS-CoV-2 proteins, sense RNA, antisense RNA, and overall SARS-CoV-2 biomass, and the down-regulated oxidative phosphorylation (OP), mitochondria transport, folate metabolism, pyruvate metabolism, and nucleotide interconversion. The overall correlation between Alpha, Delta and Omicron variants and the original IC19, respectively of the changes on these pathways was 0.60, 0.59, and 0.39, which are consistent with the order in which the variants emerged.

We next evaluated the metabolic effects of the gene and metabolite candidates for modulation identified from IC19 in the host cells infected by the different viral isolates. For gene targets, except for the agonist gene targets, the five antagonist gene targets (viz., PAICS, GART, ATIC, PPAT, PFAS) were consistent in IC19, Alpha, Delta, and Omicron isolates (**Figure 3B**). For metabolites, 19 of 20 predicted endogenous metabolites (all except mlthf) were consistent from IC19 to omicron isolates (**Figure 3C**).

Computational drug repurposing for SARS-CoV-2 infection

We first screened the FDA approved drugs based on gene targets. As five consistent gene targets are all purine synthesis enzymes (**Figure 3B**), we screened the FDA-approved drugs that not only inhibit at least one of the predicted target genes, but also have pharmacological effects

that inhibit purine synthesis. Methotrexate was identified from the DRUGBANK[28] database that met the above two criteria (**Figure 3D**).

Next, to identify candidates for drug repurposing based on metabolite targets, we overlapped drugs and compounds in DRUGBANK with molecules in Chemical Checker[23], and obtained 2,008 FDA-approved compounds in Chemical Checker. We searched for drugs that have similar network profiles as the endogenous metabolite targets (Details in **Materials and Methods**).

Six of 23 endogenous metabolites can significantly match at least one of the FDA-approved compounds by using network and pharmaceutical similarity (compound prediction score (CPS) > 0 based on network similarity, details in **Materials and Methods**), including 2−Oxoglutarate, 5-Amino-1-(5-Phospho-D-Ribosyl)Imidazole (air), 5-Amino-1-(5-Phospho-D-Ribosyl)Imidazole-4-Carboxylate (5aizc), L−Threonine, L−Proline, and L−Asparagine. At the same time, six FDA-approved drug candidates were identified (CPS>0), including Cinnamaldehyde, Bupropion, Deferiprone, Proguanil, Penicillamine, and N-acetyltyrosine (**Figure 3E**). Notably, 4 of these 6 drugs were previously studied for their antiviral functions (**Supplementary Table S11**).

In vitro experimental validation of the predicted drug candidates

To further test whether the predicted gene target and drug candidates can inhibit viral production, we selected three of the predicted drugs for subsequent validation by *in vitro* cell line experiments. These include methotrexate (an inhibitor of common drug targets), cinnamaldehyde (the top-ranked drug from common antagonist metabolites), and deferiprone (the top-ranked drug from common agonist endogenous metabolites (**Figure 3F**).

We first estimated the drug safety by performing a cytotoxicity assay (Details in **Materials and Methods**). None of the three drugs appeared to have significant cytotoxicity for the drug concentrations up to 100uM (**Figure 4A**). Immunofluorescence also showed that the level of SARS-CoV-2 N protein was significantly reduced at the concentration of 25uM for each of the three drugs(**Figure 4A**).

To measure the efficacy in viral inhibition of these three drugs, we performed the antiviral activity assay in three different lung cell types (viz., CaCo2, HPA and Huh7 cell lines) at different dosage range from 0.01uM to 100uM. As shown in **Figure 4B**, the average IC50 of methotrexate among these three cell lines was 2.0 uM (1.72uM for CaCo2, 2.03uM for HPA, and 2.17uM for Huh7). For cinnamaldehyde, the average IC50 was 3.9uM (2.59uM for CaCo2, 3.73uM for HPA, and 5.43uM for Huh7). For deferiprone, the average IC50 was 2.59uM (1.97uM for CaCo2, 2.07uM for HPA, and 3.72 for Huh7). Remdesivir was used as a positive control, which had an average IC50 of 0.83uM as measured (**Figure 4B**).

Together, these results showed that all three tested drugs have a significant anti-viral effect with the IC50 of SARS-CoV-2 ranging from 2.0uM to 3.9uM, clearly supporting that vhMM is effective in computational drug repurposing for anti-viral applications.

Analysis of the predicted repurposing drugs on real-world patient data

We next attempted to analyze the effect of these three drugs in a real-world setting. Methotrexate had an IC50 of 2.0uM, and the effective dosage was estimated at 40 mg/day (Details in **Materials and Methods)**, which is much higher than the usage of the drug for autoimmune-related diseases (< 20mg/week)[36]. Deferiprone had an IC50 of 2.59uM and an

estimated dosage of 55mg/day. However, we could not obtain enough data in ACT Network[37], presumably because deferiprone is an orphan drug for the treatment of iron overload in thalassaemia[38].

Cinnamaldehyde is the main active component in cinnamon (~3% cinnamaldehyde)[39]. It had an IC50 of 3.9uM and an estimated cinnamon equivalent dosage of 0.59 gram/day. On the other hand, cinnamon supplements typically have a daily dosage of 2-4 grams. We analyzed the incidences of COVID-19 in the ACT Network with respect to cinnamon usage. Since cinnamon is mainly used in supportive care for diabetic patients, we used patients with diabetes as the control group. A retrospective cohort of 410,645 individuals with diabetes from five major hospitals of ACT Network was queried. There was no difference in age distribution between the two groups (**Supplementary Table S12,** Kolmogorov-Smirnov test p-value = 0.166). These included 2,460 patients taking cinnamon, with a rate of recorded SARS-CoV-2 infection of 6.5%, while the rate of infection in the control group of 408,005 patients was 10.1%. Data of the 5 hospitals consistently showed by meta-analysis that patients who took cinnamon had a significant 36% lower rate of SAR-CoV-2 infection (p = 6.1e-8, odds ratio of 0.64 and 95% CI of 0.55~0.75) (**Figure 5**). These suggest that cinnamaldehyde is a promising candidate for further investigation against COVID-19.

Discussion

In this study, we developed a novel method (vhMM) for drug screening and target identification in viral infectious diseases by integrating metabolic modeling and chemoinformatics. We applied this method to study COVID-19 and captured changes in host metabolism after viral infection. Gene and metabolite targets and six candidate drugs were identified to inhibit both original and mutated SARS-COV-2 production by modulating the host metabolism. We validated the top 3 predicted drugs using *in vitro* experiments and found that all of these candidates can effectively inhibit viral production with IC50 <4uM. In a retrospective cohort study, patients taking cinnamaldehyde showed a significant reduction in the COVID-19 infection rate.

Many viruses, including SARS-CoV-2, depend on the cell metabolism of the infected host for viral replication[40, 41]. vhMM was designed to computationally predict antiviral compounds by modulating the host. In contrast to the commonly used approach of targeting viral proteins[42, 43], vhMM aims to target host metabolism by rescuing or partially rescuing the metabolic dysfunction in host cells after viral infection. We found that the suppression of mitochondria function is one of the major metabolic changes after SARS-CoV-2 infection, which was supported by the recent study of rodent and patient tissues [29]. In addition, the results are consistent in three independent studies from three different laboratories on most pandemic viral variants (alpha, delta and omicron), indicating that vhMM is robust and likely able to tolerate or at least partially tolerate viral mutations. Further, the top candidates were validated by *in vitro* cell line experiments as well as by the analysis of real-world patient data. These results suggest that vhMM is an effective computational method for anti-viral applications.

We performed validation experiments on three predicted candidate drugs, methotrexate, cinnamaldehyde, and deferiprone, and strikingly, all these drugs showed anti-viral activity in multiple lung cell lines. Given that purine synthesis is essential for viral RNA replication and has been approved in other viral diseases[44-46], and a recent study showed that inhibiting the host

nucleotide synthesis can effectively block the SARS-COV-2 replication[47], our results further confirmed, at least *in vitro*, that inhibition of purine synthesis by methotrexate can also inhibit the viral production of SARS-CoV-2. Deferiprone is an iron-chelating drug to treat iron overload from blood transfusions in thalassemia[48]. Here we found that deferiprone can also inhibit viral production in a way mimicking 2-oxoglutarate, which may involve modulating cellular redox stress, energy production, or nitrogen metabolism[49, 50].

Cinnamaldehyde, the main active component of Cinnamon, has been previously investigated for its potential beneficial metabolic effects, e.g., increasing glucose uptake and improving insulin sensitivity[51], and cinnamon is sometimes recommended as a supplement for diabetic patients[52]. Here we demonstrated that cinnamaldehyde could inhibit SARS-COV-2 replication by inhibiting intermediate molecules in purine biosynthesis as predicted by vhMM. This is consistent with structure-based prediction of protein targets of cinnamaldehyde in ChEMBL[53]. Retrospective analysis of patient data showed consistent results in patients taking oral cinnamon supplements. Interestingly, the results of a Phase 3 trial (COVID-OUT) recently showed that outpatient treatment with metformin during the initial infection significantly reduced the incidence of long COVID[54], raising the possibility of modulating host metabolism toward homeostasis to prevent the risk of long COVID.

There are still several limitations in our study. First, we did not consider signaling pathways in vhMM, which may result in missing important drug targets and candidates. Second, although the three compounds predicted here have been validated in vitro cell lines, and one of them has been further validated *in vivo* in a large-scale cohort, clinical trials are essential to evaluate their effect in the treatments of COVID-19. Third, the mechanisms of anti-viral activities of these three experimentally supported compounds require further investigation.

Conclusions

We present a new computational method, vhMM, to evaluate the disturbances of metabolism in virus-infected host cells and to predict repurposing drugs to modulate the host metabolism against viral infections. vhMM was applied to analyze the host metabolism hijacked by SARS-CoV-2 and, importantly, predicted and validated gene and metabolite targets and drug candidates *in vitro* and using real-world data. These results support further drug discovery and repurposing developments to modulate host metabolism in COVID-19 and other viral diseases.

Methods

Dataset collections

Datasets from several sources were utilized to develop the computational model for studying the host metabolic response after SARS-CoV-2 infection. These included the genome-wide metabolic model of human cells[55], information on the genomic and proteomic sequences of the SARS-CoV-2 virus[24], RNA-sequencing data of three cell lines (A549, Calu3, and NHBE) infected by the original variant[26], Calu3 cell line infected by the Alpha variant[34] and Calu3 cell line infected by the Delta variant and Omicron variant (BA.5 variant)[35], metabolic uptake dataset[56], chemical information of FDA approved drugs from DrugBank[28], and the

harmonized chemical and biological profiles of ~800,000 small molecules from Chemical Checker[23].

Genome wide precision metabolic modeling

Construction of virus-host metabolic modeling models. First**,** 28 viral protein production reactions, RNA production reactions, and lipid synthesis reactions were incorporated into the human metabolic model (**Supplementary Table S13**). The viral biomass reaction was then constructed using the structural composition from the experimental data of SARS-CoV-2[25]. The viral biomass reaction is:

2.0 YP_009724393[c] + 1.0 YP_009724397[c] + 0.1 YP_009724392[c] + 0.3 YP_009724390[c] + 0.01 COVID_RNA_BS_pos[c] + 0.01 COVID_RNA_BS_neg[c] + 0.001 COVID_lipids_v[c]

Metabolic modeling. We used our recently developed genome-wide precision metabolic modeling method, GPMM, to perform the genome-wide metabolic modeling[19]. Briefly, GPMM integrates the estimated protein abundance from gene expression and enzymatic kinetic parameters into the generic human metabolic model as upper bounds based on Michaelis–Menten kinetics. In addition, the nutrient uptake fluxes of cell lines are derived from the literature[56] and the lower bound of other exchanges was set at zero. The flux variability analysis (FVA) is conducted to construct the tissue-specific models for each cell line using the FastMM toolbox[27].

To obtain the flux change after COVID-19 infection, we performed Monte-Carlo (MCMC) simulations using the Cobra 3.0 toolbox[57]. Since ATP production is essential for all cells, we constrained the low bound of ATP production as 90% of its optimized value, similar to previous studies[58]. Similarly, the lower bound of the fluxes of host biomass and COVID-19 production biomass was set at 90% for the normal and SARS-COV-2 infected cells. Thus, the MCMC sampling provided thousands of feasible fluxes for each reaction but still maintained the feasible ATP production and biomass reaction for the normal and infected cells. The flux changes between normal and infected cells were calculated using the Limma package [59] based on the averaged values of the MCMC results.

Identifying metabolic pathway changes. The differential abundance score (DA score) was calculated using the previously published method[60]. For each metabolic pathway (i), the DA score ($\mathrm{DA_i}$) can be calculated as following:

$$\mathrm{DA_i} = \frac{\textbf{\# up regulated fluxes} - \textbf{\# down regulated fluxes}}{\textbf{Total reactions in } i\boldsymbol{th} \textbf{ subsystem}} \quad (1)$$

All-against-all gene knockout analysis. *In silico* knockout analysis was performed to obtain the effect of each gene knockout on each reaction by using the function of "FastMM_singleGeneKO" in our recently developed FastMM toolbox[27]. We thus obtained an all-against-all gene knockout matrix (G^{KO}), where rows and columns represented the genes and reactions, respectively. As the flux of transport was not constrained in GPMM due to the lack of enzymatic parameters[19], we removed the knockout results of transporters.

Identification of gene targets. To identify the gene targets for modulation, we first constructed a gene effective matrix($G^{(EM)}$), which can be calculated as:

$$G_{i,j}^{(EM)} = G_{i,j}^{(KO)} \times sign(log2FC_j) \times L_j \quad (2)$$

where i and j represent the ith gene and the jth reaction, and $log2FC_j$ and L_j are the log2 fold change and logical of (significance p<0.05 AND log2 fold change >0.5) in the jth flux, respectively.

Then, we calculated the gene effective score (GES) by summing the effective values in $G^{(EM)}$ and calculated as the following:

$$\mathrm{GES_i} = \sum_{j=1}^{n} \mathrm{G}_{\mathrm{I,j}}^{(\mathrm{EM})} \quad (3)$$

From equation (2), the value of GES >0 or <0 indicates that knocking out this gene can either rescue or enhance the flux changes in the host cells due to infection. To be stringent, we only considered GES > 3 or GES < -3 as potential candidates for antagonist targets or agonist targets, respectively. To obtain robust results, the candidates from each of the three cell types (A549, Calu3 and NHBE) were compared, and only those identified in all the cell lines were designated as gene targets for modulation.

All-against-all metabolite knockout analysis. The knockout analysis was conducted using the function of "FastMM_singleMetKO" in the FastMM toolbox to obtain the all-against-all metabolite knockout matrix($M^{(KO)}$), where row and column represent the gene and reaction, respectively.

Identification of endogenous metabolite targets. Similar to the gene targets, we obtained a metabolite effective matrix($M^{(EM)}$), which was calculated as:

$$M_{i,j}^{(EM)} = M_{i,j}^{(KO)} \times sign(log2FC_j) \times L_j \quad (4)$$

Where $M_{i,j}^{(EM)}$ represented the effect score of the ith metabolite on the jth reaction.

Then, we calculated the overall metabolite effective score (MES) by summing the effective values in $M^{(EM)}$:

$$\mathrm{MES_i} = \sum_{j=1}^{n} I \quad . \quad (5)$$

Similar to the gene targets, we only consider the MES > 3 or MES < -3 as the antagonist or agonist candidates, respectively, and the final list of metabolite targets was obtained by also limiting to the candidates consistently found in each of the three cell types.

<u>Drug repositioning using chemoinformatics</u>

To identify candidate drugs modulating the host cellular metabolism, we reason drugs that have similar network and pharmacological profiles of agonist metabolites or opposite profiles of antagonist metabolites can potentially rescue the COVID-19 metabolic change.

First, we mapped each of the antagonist and agonist metabolites to the Chemical Checker (CC) database and obtained the normalized the fingerprint for 25 different types of molecular features[23]. For each gene target, compounds in CC were also identified that either inhibit or activate the gene, which constitutes the profile of the gene.

Second, we calculated the fingerprint correlations between these metabolites and the ~800,000 small molecules in CC database to obtain the background correlation distribution. This correlation matrix can be written as $C_{i,j}^{(k)}$, represented the Pearson correlation value of *i*th metabolites and *j*th molecules in kth feature. The value of $C_{i,j}^{(k)}$ ranges from -1 to 1, where the negative and positive values represent the opposite and similar feature between the two molecules. We used the maximum likelihood method ('fgev' function in R 'evd' package) to fit the generalized extreme value distribution and estimated the location parameter μ, the scale parameter σ and the shape parameter ξ for each metabolite for each molecular feature. The extreme value distribution of background has been used in our previously developed anti-cancer prediction method [61].

Third, for a given molecule *m*, the one-tailed similarity p-value between m and the screened metabolite *i* ($p_i^{Ik)}$) can be calculated as following:

$$p_i^{(k)} = \begin{cases} 1 - F\left(C_{i,m}^{(k)}; \mu_i^{(k)}, \sigma_i^{(k)}, \xi_i^{(k)}\right), & if \;\; C_{i,m}^{(k)} > 0 \\ F\left(C_{i,m}^{(k)}; \mu_i^{(k)}, \sigma_i^{(k)}, \xi_i^{(k)}\right), & if \; C_{i,m}^{(k)} \leq 0 \end{cases} \tag{6}$$

Where $F\left(C_{i,m}^{(k)}; \mu_i^{(k)}, \sigma_i^{(k)}, \xi_i^{(k)}\right)$ represents the cumulative function of generalized extreme value distribution. $C_{i,m}^{(k)}$ represents the fingerprint correlation between the give molecule *m* and the metabolites *i* in the feature k. $\mu_i^{(k)}, \sigma_i^{(k)}, and \; \xi_i^{(k)}$ represent the location, scale and the shape parameters of the generalized extreme distribution.

Finally, for each drug compound, we calculate the compound prediction score (CPS) to rank the similarity between the drug compound and the gene and metabolite targets based on three network features: mechanism of action of the compounds (B1 in CC), and pathway features (C2 and C3 in CC), which can be calculated as:

$$CPS = \max_{i \in [1,n]} \left[-\alpha_i * log10 \left(p_i^{(B1)} \times p_i^{(C2|C3)} \right) \right] \tag{7}$$

Where *n* is the total number of antagonist and agonist metabolites, α_i is a discriminate factor. When both $p_i^{(B1)}$ and $p_i^{(C2|C3)}$ are smaller than p-cutoff (e.g., 0.01), $\alpha_i = 1$, else $\alpha_i = 0$. A compound with the CPS >0 was considered a candidate for repurposing.

We retrieved the FDA-approved compounds from DrugBank[28]. After filtering the drugs that were not included in the CC database, we obtained six candidate drugs for anti-COVID-19.

In vitro **experimental validation**

The SARS-CoV-2 (NMDCN000HUI) was propagated and titrated on Vero E6 cells (ATCC, no. 1586). Human pulmonary alveolar epithelial cell line (HPAEpiC) was purchased from the ScienCell Research Laboratory (San Diego, CA). Human hepatocarcinoma cell line Huh7 were purchased from Procell Life Science & Technology Co., Ltd (Wuhan, China). Human colorectal adenocarcinoma cell line Caco-2 was purchased from Cell Bank, Chinese Academy of Sciences. All the cells were cultured in high glucose DMEM medium with 4.5 mM L-glutamine (Gibco) contains with 10% FBS (Gibco) and 1% penicillin–streptavidin (Gibco). All work with SARS-CoV-2 was conducted in a BSL-3 facility at the Key Laboratory of Animal Models and Human

Disease Mechanisms of the Chinese Academy of Sciences, Kunming Institute of Zoology (Kunming, China).

Cytotoxicity assay. The cytotoxicity of compounds on HPAEpiC cells and Huh7 cells was determined by CCK8 assay. Briefly, 8×10^4 per well HPAEpiC or 4×10^4 per well Huh7 cells were respectively seeded in 96-well plates and incubated at 37°C, 5% CO2 overnight. When the cells grew to more than 90% confluence, they were incubated with or without series diluted compounds in 96-well cell culture plates and further incubated for 72 hours. 10 μL CCK8 (Beyotime) was added to each well at 37°C, and one hours later, the optical absorbance was measured by ELx800 reader (Bio-Tek) at 450 nm/630 nm. 50% cytotoxicity concentration (CC_{50}) was calculated.

Immunofluorescence experiment (IFA). 2×10^5 cells Caco-2 were seeded on glass coverslips pretreated with TC (Solarbio) in 24-well plates to reach 90% confluency and infected with virus at an MOI of 0.02. Meanwhile, the test compounds were added to the wells. After 1 hour, the supernatant was discarded, and the wells were washed 3 times with PBS and replaced with fresh medium containing drug compounds. After 48 hours, cells were fixed in 4% paraformaldehyde and subjected to IFA.

Antiviral activity assay. 1.6×10^5 cells of HPAEpiC or 8×10^4 cells of Huh7 or Caco-2 were respectively seeded in 48-well plates and grown overnight. HPAEpiC cells, Huh7 cells, and Caco-2 cells were infected at an MOI of 1, 0.1and 0.02. At the same time, the test compounds were added to the wells with different concentrations. One hour later, the drug-virus mixture was removed, and cells were washed 3 times to remove the free virus with PBS and replaced with fresh medium containing compounds. 48 hours later, the supernatants were collected, and viral RNA was extracted by using a High pure Viral RNA Kit (Roche), RT-qPCR analysis was performed. Viral RNA was quantified by THUNDERBIRD® Probe One-step qRT-PCR Kit (Toyobo). TaqMan primers for SARS-CoV-2 are 5'-GGGGAA’TTCTCCTGCTAGAAT-3' and 5’’CAGACA’TTTGCTCTCAAGCTG-3' with S’RS-CoV-2 probe FAM-TTGCTGCTGCTTGACAGATT-TAMRA-3'. The I’50 values were calculated by using a dose-response model in GraphPad Prism 7.0 software.

In vivo retrospective cohort study of the ACT network

A rough estimation of the dosage of the repurposed. The drug dose was estimated using the formula by $MW \times IC50 \times V \times \frac{24}{HL}/1000$, where MW is the molecular weight (unit g/mol), V is the volume of liquid in adults (12L for 60 kg adult), HL is the half-life time (in hours) of the given drug. IC50 is the half maximal inhibitory concentration (in uM). For methotrexate, HL is approximately 6.5 hours[28], and we estimated the dose of 40 mg/day ($454.44 \times 2 \times 12 \times \frac{24}{6.5}/1000$). For deferiprone, the HL is 1.9 hours [28], and the estimated dose was 55mg/day ($139.15 \times 2.59 \times 12 \times \frac{24}{1.9}/1000$). For cinnamaldehyde, the HL is 8.7 hours[62], and the estimated dose is 17.06 mg/day ($132.16 \times 3.9 \times 12 \times \frac{24}{8.7}/1000$). As cinnamaldehyde is the major active component in cinnamon (2.89% cinnamaldehyde)[39], the estimated cinnamon dose is 17.06 mg/day /0.0289 = 0.59 gram/day.

This retrospective cohort study utilized the real-world patient data of the Accrual to Clinical Trials (ACT) network of 35 Clinical and Translational Science Awards (CTSA)-affiliated

hospitals[37]. Since cinnamon is mainly used in supportive care for diabetic patients, we queried among patients with a diagnosis of diabetes between 01/01/2020 and 09/09/2022 whether they used cinnamon and whether they had a confirmed case of COVID-19.

The query criteria were the following: i) Diabetes: ICD-9: 250, ICD-10: E08-E13. ii) COVID-19: confirmed cases under CDC case definition, i.e., diagnostic laboratory tests results as active infection test positive. iii) Cinnamon usage: Chromium Picolinate / Cinnamon Bark (1313956), Cinnamon Allergenic Extract (899673), Cinnamon Bark (477053), Cinnamon Preparation (285245).

To obtain robust results, we only included in the analysis data from five hospitals where at least 200 patients took cinnamon. In total, 410,645 individuals with diabetes from these five hospitals were studied: 2,460 patients who took cinnamon were in the case group, and the rest were in the control group. For each hospital, the COVID-19 infection rates were calculated for the case and control groups, and meta-analysis was conducted to estimate the effect of cinnamon usage on COVID-19 infection rate.

Availability of data and materials

The code and processed data in this manuscript can be available from http://github.com/GonghuaLi/vhMM.

Acknowledgments

This work was supported by grants from Open Medicine Foundation and the Stupski Foundation (WX), the CAS Project for Young Scientists in Basic Research (YSBR-076), Yunnan Applied Basic Research Project (202101AS070058), High-level Talent Promotion and Training Project of Kunming (Spring City Plan; 2020SCP001), National Key R & D Program of China (2022YFC2303700), Yunnan Key Research and Development Program (202103AC100005) and Yunling Scholar of Yunnan Province.

Author contributions

GHL, QPK, and WX conceived and designed the study. GHL and WX designed the computational method. GHL developed the computational method, and GHL and FH collected the datasets and performed the analysis. YTZ designed the validation experiments, and RHL and XYL conducted the validation experiments. PL, GHL and WX performed the analysis of real-world data. GHL, FH, CJC, and WX performed the statistical analysis. GHL, FH, RHL, PL, and WX drafted the manuscript. WX, GHL, FH, RHL, PL, WHX, JFH, QPK, and YTZ revised the manuscript. All authors read and approved the final manuscript.

Ethics declarations

Ethics approval and consent to participate

Not applicable.

Consent for publication

Not applicable.

Competing interests

The authors declare that they have no competing interests.

Figure legends:

Figure 1: A Flowchart of viral-host Metabolic Modeling (vhMM). Step 1, Model reconstruction of human cells after viral infection. Step 2, Genome-wide precision metabolic modeling to identify metabolic changes after infection and in silicon genome-wide knock-outs to identify genes and metabolites as targets for modulation. Step 3, Drug repurposing by identifying candidate drugs that mimic the molecular characteristics of the gene and metabolite targets.

Figure 2: Prediction of gene and endogenous metabolite targets. (A) Correlation between the predicted viral load by vhMM and the experimentally measured viral load ($r = 0.75$, $p = 0.003$). (B) Heatmap of changes of metabolic pathways after SARS-COV-2 infection in three cell lines (Calu3, ACE2-induced A549, and NHBE). Note: ***, **, *, and . represent the false discovery rate (FDR) of <0.001, <0.01, < 0.05, and < 0.1, respectively. (C) Gene effective scores of predicted gene targets in the three infected cell lines. (D) Metabolite effective scores of predicted endogenous metabolites as targets in the three infected cell lines.

Figure 3: Prediction of repurposing drugs among IC19, Alpha, Delta and Omicron variants. (A) Heatmap of metabolic pathway changes in IC19, Alpha, Delta, and Omicron variant infected cells. Note: ***, **, *, and . represent FDR of <0.001, <0.01, < 0.05, and < 0.1, respectively. (B) Gene effective scores of predicted gene targets in different viral isolates. (C). Metabolite effective scores of predicted endogenous metabolite targets in different viral isolates. (D) Drug repurposing by requiring the inhibition of at least one antagonist gene target and the inhibition of purine synthesis. (E) Drug repurposing based on metabolite targets. Blue and red colors represent antagonist and agonist endogenous metabolites, respectively. The metabolites and predicted drugs are listed in descending order based on the metabolite effective score (MES) and the compound prediction score (CPS), respectively. (F) Drugs selected for in vitro validation. Methotrexate is an FDA-approved drug and is predicted to inhibit the antagonist gene targets and pathway, while Cinnamaldehyde and Deferiprone are the top-ranked drugs from antagonist and agonist endogenous metabolites, respectively.

Figure 4: Experimental validation of Methotrexate, Cinnamaldehyde, and Deferiprone. (A) Immunofluorescence experiment of the three predicted drugs. Different drug concentrations (25uM, 50uM, and 100uM) were assayed for each of the drugs. (B) Antiviral activity assay of the three predicted drugs and a positive control (remdesivir). Three lung cell lines (CaCo2, HPA, and Huh7) were used to test the antiviral activity of each drug.

Figure 5: Analysis of a real-world patient dataset on cinnamon. Cinnamaldehyde is the major active component in cinnamon. A retrospective cohort of 410,645 individuals with diabetes from five major hospitals of ACT Network was queried about incidences of COVID-19 with respect to cinnamon usage. These included 2,460 patients taking cinnamon, with a rate of recorded SARS-CoV-2 infection of 6.5%, while the rate of infection in the control group of 408,005 patients was 10.1%. Data from the five hospitals consistently showed that patients who took cinnamon had a significantly lower rate of SAR-CoV-2 infection (p = 6.1e-8, odds ratio of 0.64, and 95% CI of 0.55~0.75).

Title of table S1-S13

Table S1: Gene effective matrix of SARS-COV-2 infected ACE2-induced A549 cell line.

Table S2: Gene effective matrix of SARS-COV-2 infected Calu3 cell line.

Table S3: Gene effective matrix of SARS-COV-2 infected NHBE cell line.

Table S4: Overlapped gene targets among three cell lines.

Table S5: Overlapped gene targets among three cell lines using viral biomass reaction.

Table S6: Metabolite effective matrix of SARS-COV-2 infected ACE2-induced A549 cell line.

Table S7: Metabolite effective matrix of SARS-COV-2 infected Calu3 cell line.

Table S8: Metabolite effective matrix of SARS-COV-2 infected NHBE cell line.

Table S9: Overlapped metabolite targets among three cell lines.

Table S10: Overlapped metabolite targets among three cell lines using viral biomass reaction.

Table S11: Predicted Repurposing Drugs for Anti-COVID-19.

Table S12: Age distribution of patients in cinnamon and diabetes groups.

Table S13: The SARS-COV-2 components for vhMM.

Reference

1. Harrington WN, Kackos CM, Webby RJ: **The evolution and future of influenza pandemic preparedness.** *J Experimental molecular medicine* 2021, **53**:737-749.
2. Sheena BS, Hiebert L, Han H, Ippolito H, Abbasi-Kangevari M, Abbasi-Kangevari Z, Abbastabar H, Abdoli A, Ali HA, Adane MM: **Global, regional, and national burden of hepatitis B, 1990–2019: a**

systematic analysis for the Global Burden of Disease Study 2019. *The lancet Gastroenterology hepatology* 2022, **7:**796-829.

3. Cascella M, Rajnik M, Aleem A, Dulebohn SC, Di Napoli R: **Features, evaluation, and treatment of coronavirus (COVID-19).** *Statpearls* 2022.
4. Murakami N, Hayden R, Hills T, Al-Samkari H, Casey J, Del Sorbo L, Lawler PR, Sise ME, Leaf DE: **Therapeutic advances in COVID-19.** *Nature Reviews Nephrology* 2022:1-15.
5. WHO: **Tracking SARS-CoV-2 variants.** *World Health Organization* 2022, **https://www.who.int/en/activities/tracking-SARS-CoV-2-variants**.
6. Eyre DW, Taylor D, Purver M, Chapman D, Fowler T, Pouwels KB, Walker AS, Peto TE: **Effect of Covid-19 vaccination on transmission of alpha and delta variants.** *New England Journal of Medicine* 2022, **386:**744-756.
7. Dejnirattisai W, Huo J, Zhou D, Zahradník J, Supasa P, Liu C, Duyvesteyn HM, Ginn HM, Mentzer AJ, Tuekprakhon A: **SARS-CoV-2 Omicron-B. 1.1. 529 leads to widespread escape from neutralizing antibody responses.** *Cell* 2022, **185:**467-484. e415.
8. VanBlargan LA, Errico JM, Halfmann PJ, Zost SJ, Crowe JE, Purcell LA, Kawaoka Y, Corti D, Fremont DH, Diamond MS: **An infectious SARS-CoV-2 B. 1.1. 529 Omicron virus escapes neutralization by therapeutic monoclonal antibodies.** *Nature medicine* 2022, **28:**490-495.
9. Moghadasi SA, Heilmann E, Khalil AM, Nnabuife C, Kearns FL, Ye C, Moraes SN, Costacurta F, Esler MA, Aihara H: **Transmissible SARS-CoV-2 variants with resistance to clinical protease inhibitors.** *Science Advances* 2023, **9:**eade8778.
10. Mayer KA, Stöckl J, Zlabinger GJ, Gualdoni GA: **Hijacking the supplies: metabolism as a novel facet of virus-host interaction.** *Frontiers in immunology* 2019, **10:**1533.
11. O'Brien EJ, Monk JM, Palsson BO: **Using genome-scale models to predict biological capabilities.** *Cell* 2015, **161:**971-987.
12. Väremo L, Nookaew I, Nielsen J: **Novel insights into obesity and diabetes through genome-scale metabolic modeling.** *Frontiers in physiology* 2013, **4:**92.
13. Mardinoglu A, Agren R, Kampf C, Asplund A, Uhlen M, Nielsen J: **Genome-scale metabolic modelling of hepatocytes reveals serine deficiency in patients with non-alcoholic fatty liver disease.** *Nature communications* 2014, **5:**1-11.
14. Agren R, Mardinoglu A, Asplund A, Kampf C, Uhlen M, Nielsen JJMsb: **Identification of anticancer drugs for hepatocellular carcinoma through personalized genome-scale metabolic modeling.** *Molecular systems biology* 2014, **10:**721.
15. Lewis NE, Schramm G, Bordbar A, Schellenberger J, Andersen MP, Cheng JK, Patel N, Yee A, Lewis RA, Eils RJNb: **Large-scale in silico modeling of metabolic interactions between cell types in the human brain.** *Nature biotechnology* 2010, **28:**1279-1285.

16. Cheng K, Martin-Sancho L, Pal LR, Pu Y, Riva L, Yin X, Sinha S, Nair NU, Chanda SK, Ruppin E: **Genome-scale metabolic modeling reveals SARS-CoV-2-induced metabolic changes and antiviral targets.** *Molecular systems biology* 2021, **17:**e10260.
17. Santos-Beneit F, Raškevičius V, Skeberdis VA, Bordel S: **A metabolic modeling approach reveals promising therapeutic targets and antiviral drugs to combat COVID-19.** *Scientific reports* 2021, **11:**1-11.
18. Kishk A, Pacheco MP, Sauter T: **DCcov: Repositioning of drugs and drug combinations for SARS-CoV-2 infected lung through constraint-based modeling.** *Iscience* 2021, **24:**103331.
19. Li GH, Han F, Xiao FH, Gu KSY, Shen Q, Xu W, Li WX, Wang YL, Liang B, Huang JF: **System-level metabolic modeling facilitates unveiling metabolic signature in exceptional longevity.** *Aging cell* 2022, **21:**e13595.
20. Li G-H, Dai S, Han F, Li W, Huang J, Xiao W: **FastMM: an efficient toolbox for personalized constraint-based metabolic modeling.** *BMC bioinformatics* 2020, **21:**1-7.
21. Lo Y-C, Rensi SE, Torng W, Altman RB: **Machine learning in chemoinformatics and drug discovery.** *Drug discovery today* 2018, **23:**1538-1546.
22. Kim S, Chen J, Cheng T, Gindulyte A, He J, He S, Li Q, Shoemaker BA, Thiessen PA, Yu B: **PubChem in 2021: new data content and improved web interfaces.** *Nucleic acids research* 2021, **49:**D1388-D1395.
23. Duran-Frigola M, Pauls E, Guitart-Pla O, Bertoni M, Alcalde V, Amat D, Juan-Blanco T, Aloy P: **Extending the small-molecule similarity principle to all levels of biology with the Chemical Checker.** *Nature Biotechnology* 2020, **38:**1087-1096.
24. Ostaszewski M, Niarakis A, Mazein A, Kuperstein I, Phair R, Orta-Resendiz A, Singh V, Aghamiri SS, Acencio ML, Glaab E: **COVID19 Disease Map, a computational knowledge repository of virus–host interaction mechanisms.** *Molecular systems biology* 2021, **17:**e10387.
25. Bar-On YM, Flamholz A, Phillips R, Milo R: **Science Forum: SARS-CoV-2 (COVID-19) by the numbers.** *elife* 2020, **9:**e57309.
26. Blanco-Melo D, Nilsson-Payant BE, Liu W-C, Uhl S, Hoagland D, Møller R, Jordan TX, Oishi K, Panis M, Sachs D: **Imbalanced host response to SARS-CoV-2 drives development of COVID-19.** *Cell* 2020, **181:**1036-1045. e1039.
27. Bhadra M, Howell P, Dutta S, Heintz C, Mair WB: **Alternative splicing in aging and longevity.** *Human genetics* 2020, **139:**357-369.

28. Wishart DS, Feunang YD, Guo AC, Lo EJ, Marcu A, Grant JR, Sajed T, Johnson D, Li C, Sayeeda Z: **DrugBank 5.0: a major update to the DrugBank database for 2018.** *Nucleic acids research* 2018, **46:**D1074-D1082.
29. Guarnieri JW, Dybas JM, Fazelinia H, Kim MS, Frere J, Zhang Y, Soto Albrecht Y, Murdock DG, Angelin A, Singh LN: **Core mitochondrial genes are down-regulated during SARS-CoV-2 infection of rodent and human hosts.** *Science Translational Medicine* 2023, **15:**eabq1533.
30. Mifsud EJ, Hayden FG, Hurt AC: **Antivirals targeting the polymerase complex of influenza viruses.** *Antiviral research* 2019, **169:**104545.
31. Robinson AD, Eich M-L, Varambally S: **Dysregulation of de novo nucleotide biosynthetic pathway enzymes in cancer and targeting opportunities.** *Cancer letters* 2020, **470:**134-140.
32. Hoffmann H-H, Kunz A, Simon VA, Palese P, Shaw ML: **Broad-spectrum antiviral that interferes with de novo pyrimidine biosynthesis.** *Proceedings of the National Academy of Sciences* 2011, **108:**5777-5782.
33. DeGrace MM, Ghedin E, Frieman MB, Krammer F, Grifoni A, Alisoltani A, Alter G, Amara RR, Baric RS, Barouch DH: **Defining the risk of SARS-CoV-2 variants on immune protection.** *Nature* 2022, **605:**640-652.
34. Thorne LG, Bouhaddou M, Reuschl A-K, Zuliani-Alvarez L, Polacco B, Pelin A, Batra J, Whelan MV, Hosmillo M, Fossati A: **Evolution of enhanced innate immune evasion by SARS-CoV-2.** *Nature* 2022, **602:**487-495.
35. Bouhaddou M, Reuschl A-K, Polacco BJ, Thorne LG, Ummadi MR, Ye C, Ramirez RR, Pelin A, Batra J, Jang GMJb: **Global landscape of the host response to SARS-CoV-2 variants reveals viral evolutionary trajectories.** *bioRxiv* 2022:2022.2010. 2019.512927.
36. Cronstein BN: **Low-dose methotrexate: a mainstay in the treatment of rheumatoid arthritis.** *Pharmacological reviews* 2005, **57:**163-172.
37. Visweswaran S, Becich MJ, D'Itri VS, Sendro ER, MacFadden D, Anderson NR, Allen KA, Ranganathan D, Murphy SN, Morrato EH: **Accrual to Clinical Trials (ACT): a clinical and translational science award consortium network.** *JAMIA open* 2018, **1:**147-152.
38. Kontoghiorghes GJ, Neocleous K, Kolnagou A: **Benefits and risks of deferiprone in iron overload in thalassaemia and other conditions.** *Drug Safety* 2003, **26:**553-584.
39. He Z-D, Qiao C-F, Han Q-B, Cheng C-L, Xu H-X, Jiang R-W, But PP-H, Shaw P-C: **Authentication and quantitative analysis on the chemical profile of cassia bark (cortex cinnamomi) by high-pressure liquid chromatography.** *Journal of Agricultural Food Chemistry* 2005, **53:**2424-2428.
40. Mullen PJ, Garcia G, Purkayastha A, Matulionis N, Schmid EW, Momcilovic M, Sen C, Langerman J, Ramaiah A, Shackelford DB: **SARS-CoV-2 infection rewires host cell metabolism and is potentially susceptible to mTORC1 inhibition.** *Nature communications* 2021, **12:**1-10.

41. Thaker SK, Ch'ng J, Christofk HR: **Viral hijacking of cellular metabolism.** *BMC biology* 2019, **17:**1-15.

42. Vora SM, Fontana P, Mao T, Leger V, Zhang Y, Fu T-M, Lieberman J, Gehrke L, Shi M, Wang L: **Targeting stem-loop 1 of the SARS-CoV-2 5′ UTR to suppress viral translation and Nsp1 evasion.** *Proceedings of the National Academy of Sciences* 2022, **119:**e2117198119.

43. Zhang G, Cong Y, Liu F-L, Sun J, Zhang J, Cao G, Zhou L, Yang W, Song Q, Wang F: **A nanomaterial targeting the spike protein captures SARS-CoV-2 variants and promotes viral elimination.** *Nature Nanotechnology* 2022:1-11.

44. Li J, Zhao J, Xu S, Zhang S, Zhang J, Xiao J, Gao R, Tian M, Zeng Y, Lee K: **Antiviral activity of a purine synthesis enzyme reveals a key role of deamidation in regulating protein nuclear import.** *Science advances* 2019, **5:**eaaw7373.

45. Wang Y, Wang W, Xu L, Zhou X, Shokrollahi E, Felczak K, Van Der Laan LJ, Pankiewicz KW, Sprengers D, Raat NJ: **Cross talk between nucleotide synthesis pathways with cellular immunity in constraining hepatitis E virus replication.** *Antimicrobial agents chemotherapy* 2016, **60:**2834-2848.

46. Seignères B, Martin P, Werle B, Schorr O, Jamard C, Rimsky L, Trépo C, Zoulim F: **Effects of pyrimidine and purine analog combinations in the duck hepatitis B virus infection model.** *Antimicrobial agents chemotherapy* 2003, **47:**1842-1852.

47. Schultz DC, Johnson RM, Ayyanathan K, Miller J, Whig K, Kamalia B, Dittmar M, Weston S, Hammond HL, Dillen C: **Pyrimidine inhibitors synergize with nucleoside analogues to block SARS-CoV-2.** *Nature* 2022, **604:**134-140.

48. Kontoghiorghes G, Agarwal M, Grady R, Kolnagou A, Marx J: **Deferiprone for thalassaemia.** *The Lancet* 2000, **356:**428-429.

49. Harris AL: **A new hydroxy metabolite of 2-oxoglutarate regulates metabolism in hypoxia.** *Cell Metabolism* 2015, **22:**198-200.

50. Huergo LF, Dixon R: **The emergence of 2-oxoglutarate as a master regulator metabolite.** *Microbiology Molecular Biology Reviews* 2015, **79:**419-435.

51. Zhu R, Liu H, Liu C, Wang L, Ma R, Chen B, Li L, Niu J, Fu M, Zhang D: **Cinnamaldehyde in diabetes: A review of pharmacology, pharmacokinetics and safety.** *Pharmacological research* 2017, **122:**78-89.

52. Khan A, Safdar M, Ali Khan MM, Khattak KN, Anderson RA: **Cinnamon improves glucose and lipids of people with type 2 diabetes.** *Diabetes care* 2003, **26:**3215-3218.

53. Mendez D, Gaulton A, Bento AP, Chambers J, De Veij M, Félix E, Magariños MP, Mosquera JF, Mutowo P, Nowotka M: **ChEMBL: towards direct deposition of bioassay data.** *Nucleic acids research* 2019, **47:**D930-D940.

54. Carolyn T Bramante, Prof John B Buse, David M Liebovitz, Jacinda M Nicklas, Michael A Puskarich, Ken Cohen, Hrishikesh K Belani, Blake J Anderson, Jared D Huling, Christopher J Tignanelli, et al: **Outpatient treatment of COVID-19 and incidence of post-COVID-19 condition over 10 months (COVID-OUT): a multicentre, randomised, quadruple-blind, parallel-group, phase 3 trial.** *The Lancet Infectious Diseases* 2023, **Published online June 8**.
55. Brunk E, Sahoo S, Zielinski DC, Altunkaya A, Dräger A, Mih N, Gatto F, Nilsson A, Preciat Gonzalez GA, Aurich MK: **Recon3D enables a three-dimensional view of gene variation in human metabolism.** *Nature biotechnology* 2018, **36:**272-281.
56. Jain M, Nilsson R, Sharma S, Madhusudhan N, Kitami T, Souza AL, Kafri R, Kirschner MW, Clish CB, Mootha VK: **Metabolite profiling identifies a key role for glycine in rapid cancer cell proliferation.** *Science* 2012, **336:**1040-1044.
57. Heirendt L, Arreckx S, Pfau T, Mendoza SN, Richelle A, Heinken A, Haraldsdóttir HS, Wachowiak J, Keating SM, Vlasov V: **Creation and analysis of biochemical constraint-based models using the COBRA Toolbox v. 3.0.** *Nature protocols* 2019, **14:**639-702.
58. Nam H, Campodonico M, Bordbar A, Hyduke DR, Kim S, Zielinski DC, Palsson BO: **A systems approach to predict oncometabolites via context-specific genome-scale metabolic networks.** *PLoS computational biology* 2014, **10:**e1003837.
59. Ritchie ME, Phipson B, Wu D, Hu Y, Law CW, Shi W, Smyth GK: **limma powers differential expression analyses for RNA-sequencing and microarray studies.** *Nucleic acids research* 2015, **43:**e47-e47.
60. Hakimi AA, Reznik E, Lee C-H, Creighton CJ, Brannon AR, Luna A, Aksoy BA, Liu EM, Shen R, Lee W: **An integrated metabolic atlas of clear cell renal cell carcinoma.** *Cancer cell* 2016, **29:**104-116.
61. Li G-H, Huang J-F: **CDRUG: a web server for predicting anticancer activity of chemical compounds.** *Bioinformatics* 2012, **28:**3334-3335.
62. Ji B, Zhao Y, Zhang Q, Wang P, Guan J, Rong R, Yu Z: **Simultaneous determination of cinnamaldehyde, cinnamic acid, and 2-methoxy cinnamic acid in rat whole blood after oral administration of volatile oil of Cinnamoni Ramulus by UHPLC-MS/MS: An application for a pharmacokinetic study.** *Journal of Chromatography B* 2015, **1001:**107-113.

Figure 1

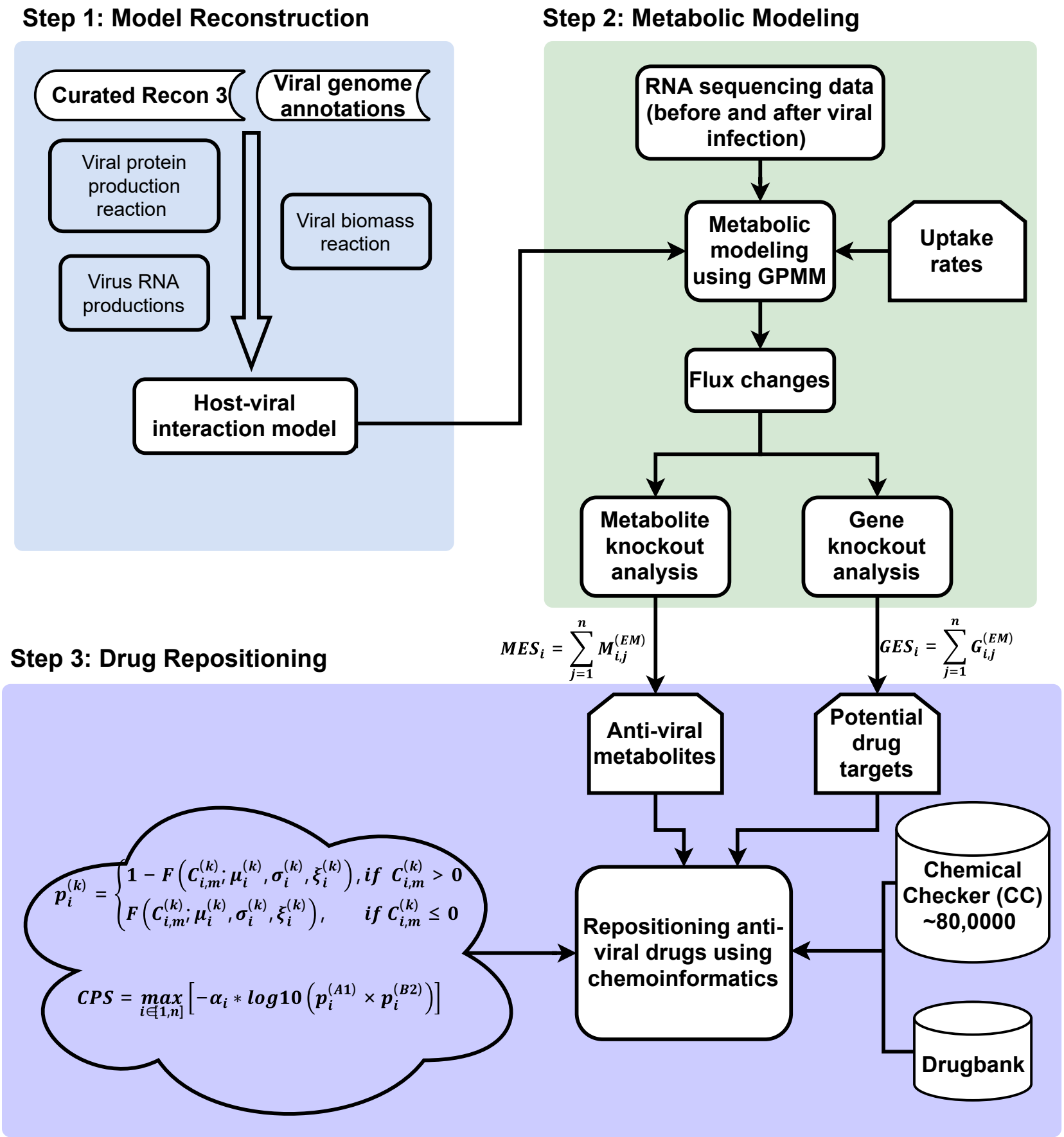
Step 1: Model Reconstruction
Curated Recon 3
Viral genome annotations
Viral protein production reaction
Viral biomass reaction
Virus RNA productions
Host-viral interaction model
Step 2: Metabolic Modeling
RNA sequencing data (before and after viral infection)
Metabolic modeling using GPMM
Uptake rates
Flux changes
Metabolite knockout analysis
Gene knockout analysis
$MES_i = \sum_{j=1}^{n} M_{i,j}^{(EM)}$
$GES_i = \sum_{j=1}^{n} G_{i,j}^{(EM)}$
Step 3: Drug Repositioning
Anti-viral metabolites
Potential drug targets
$p_i^{(k)} = \begin{cases} 1 - F\left(C_{i,m}^{(k)}; \mu_i^{(k)}, \sigma_i^{(k)}, \xi_i^{(k)}\right), if\ C_{i,m}^{(k)} > 0 \\ F\left(C_{i,m}^{(k)}; \mu_i^{(k)}, \sigma_i^{(k)}, \xi_i^{(k)}\right), \quad if\ C_{i,m}^{(k)} \leq 0 \end{cases}$
$CPS = \max_{i \in [1,n]} \left[-\alpha_i * log10\left(p_i^{(A1)} \times p_i^{(B2)}\right)\right]$
Repositioning anti-viral drugs using chemoinformatics
Chemical Checker (CC) ~80,0000
Drugbank

Figure 2

A. Predicted viral biomass and the experimental viral load

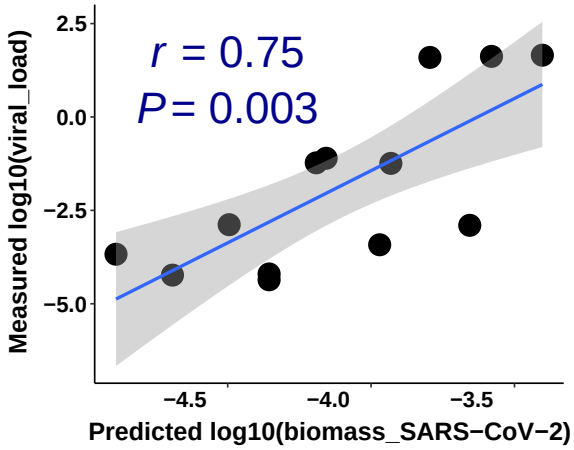

B. Changes of metabolic pathways in the three infected cell lines

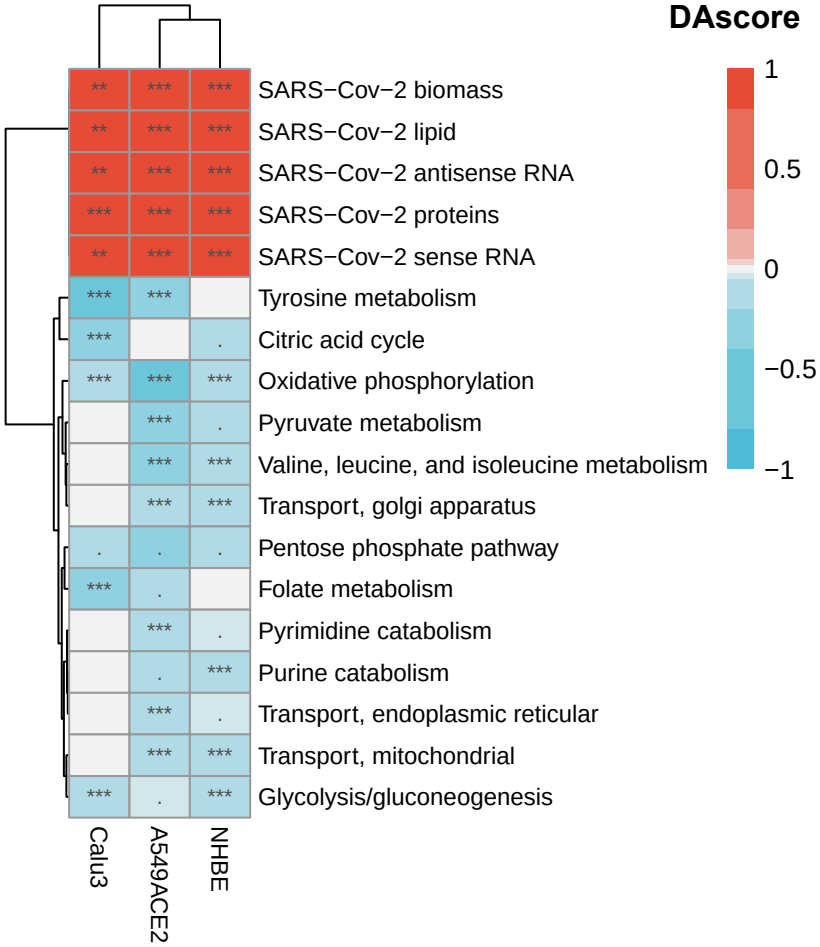

C. Predicted gene targets

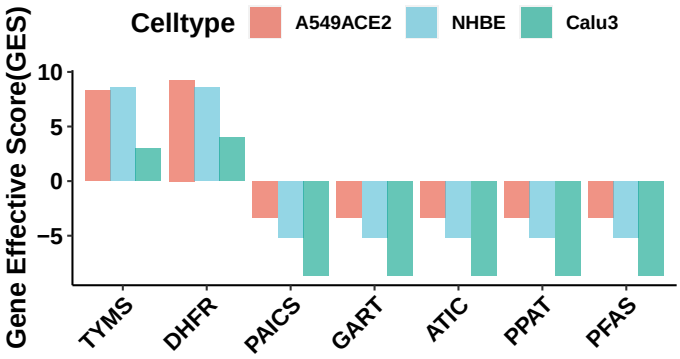

D. Predicted endogenous metabolites as targets

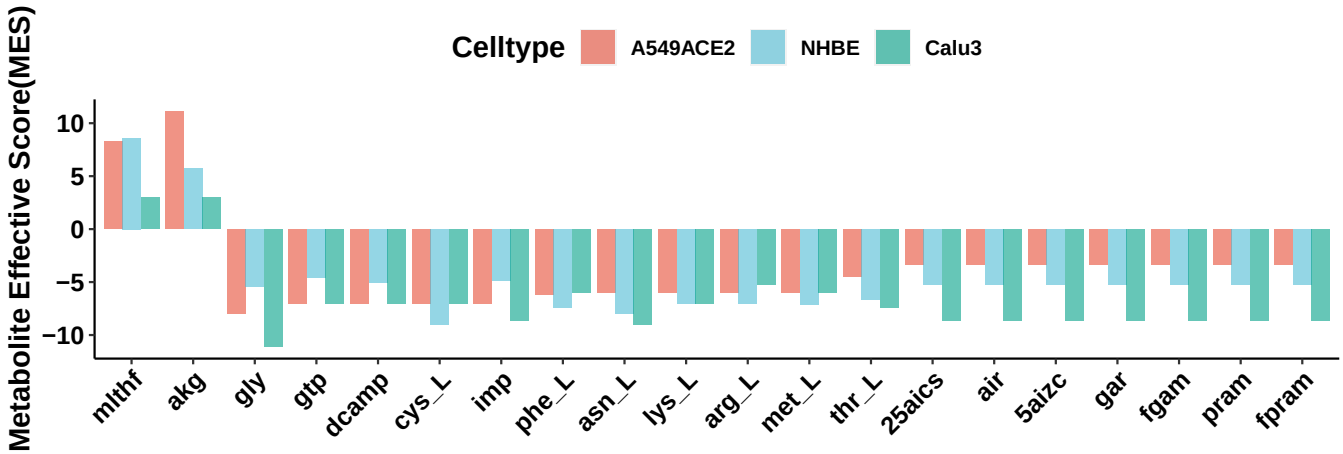

Figure 3

A. Metabolic pathway changes in different isolate infected cells

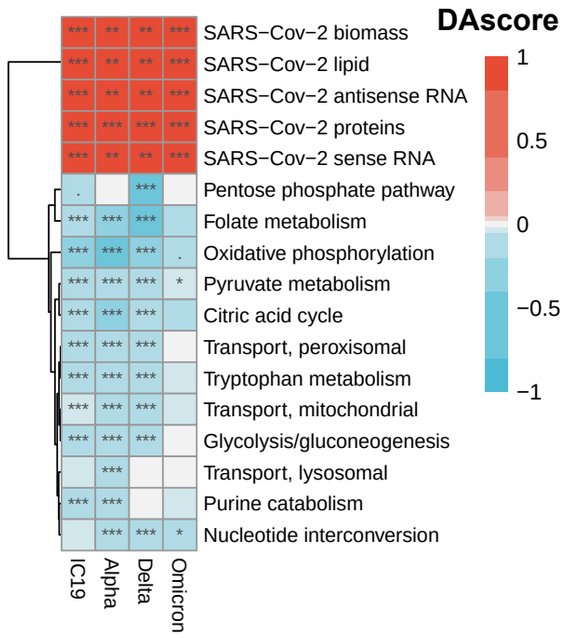

B. Predicted gene targets for different isolates

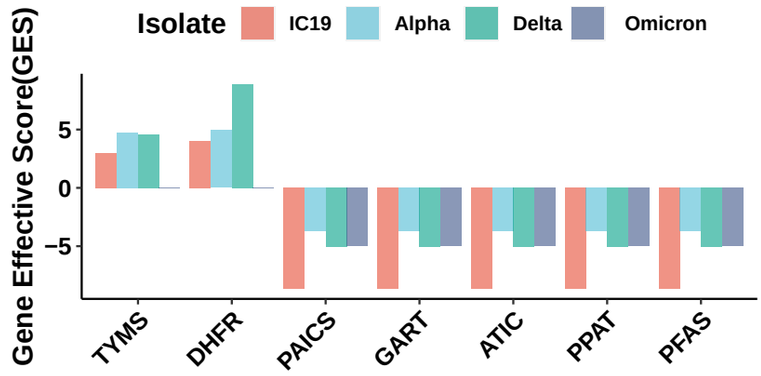

C. Predicted endogenous metabolites as targets for different isolates

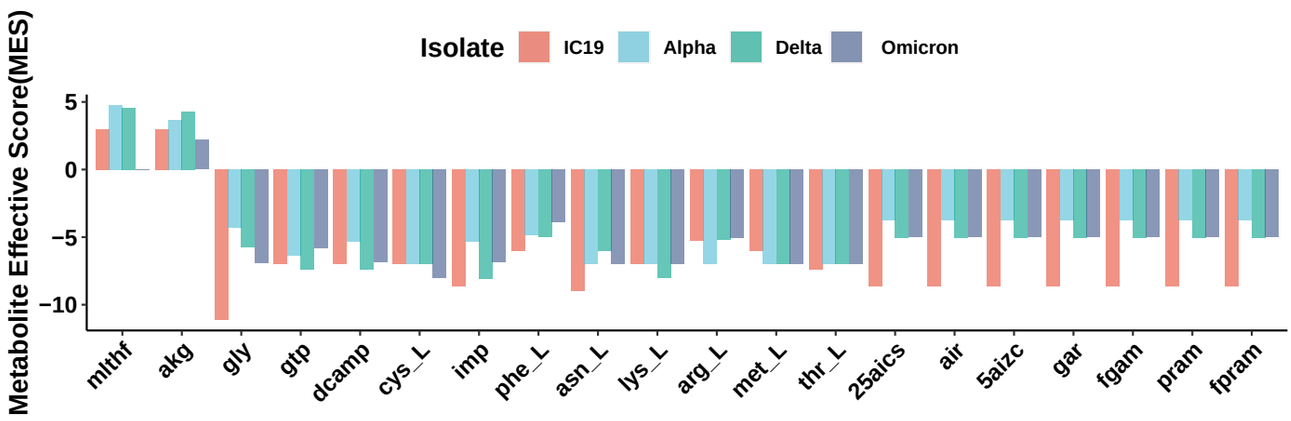

D. Drug repurposing from gene targets

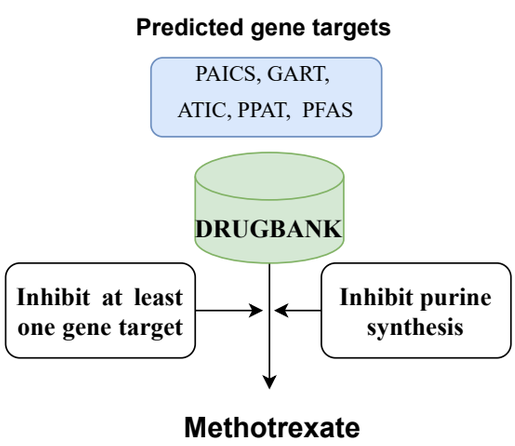

E. Drug repurposing from metabolite targets

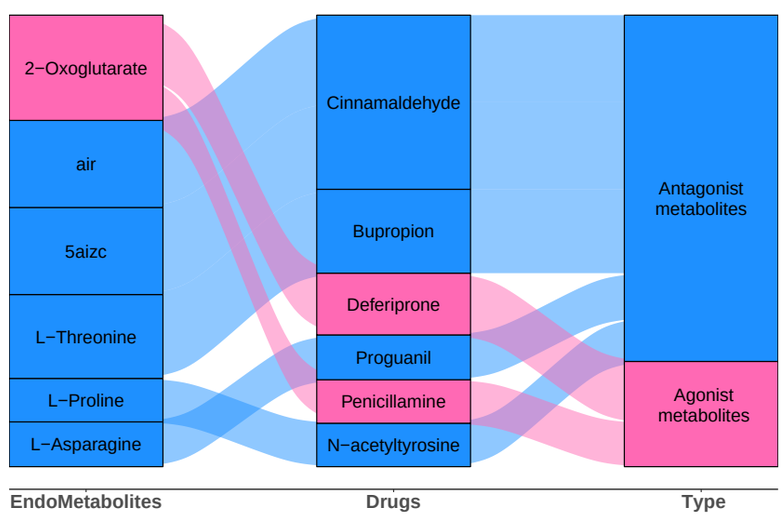

F. Drugs selected for validation

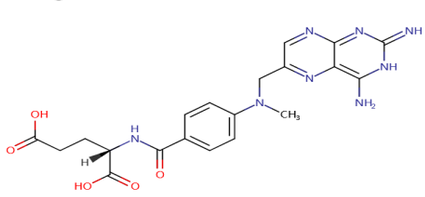

Methotrexate
(Inhibitor for overlapped antagonist gene targets)

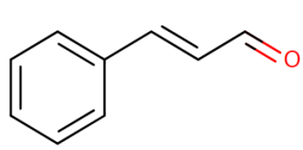

Cinnamaldehyde
(Overlapped drugs from antagonist metabolites)

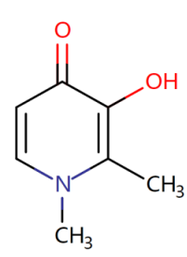

Deferiprone
(Overlapped drugs from agonist metabolites)

Figure 4

A. Immunofluorescence experiment of the three predicted drugs

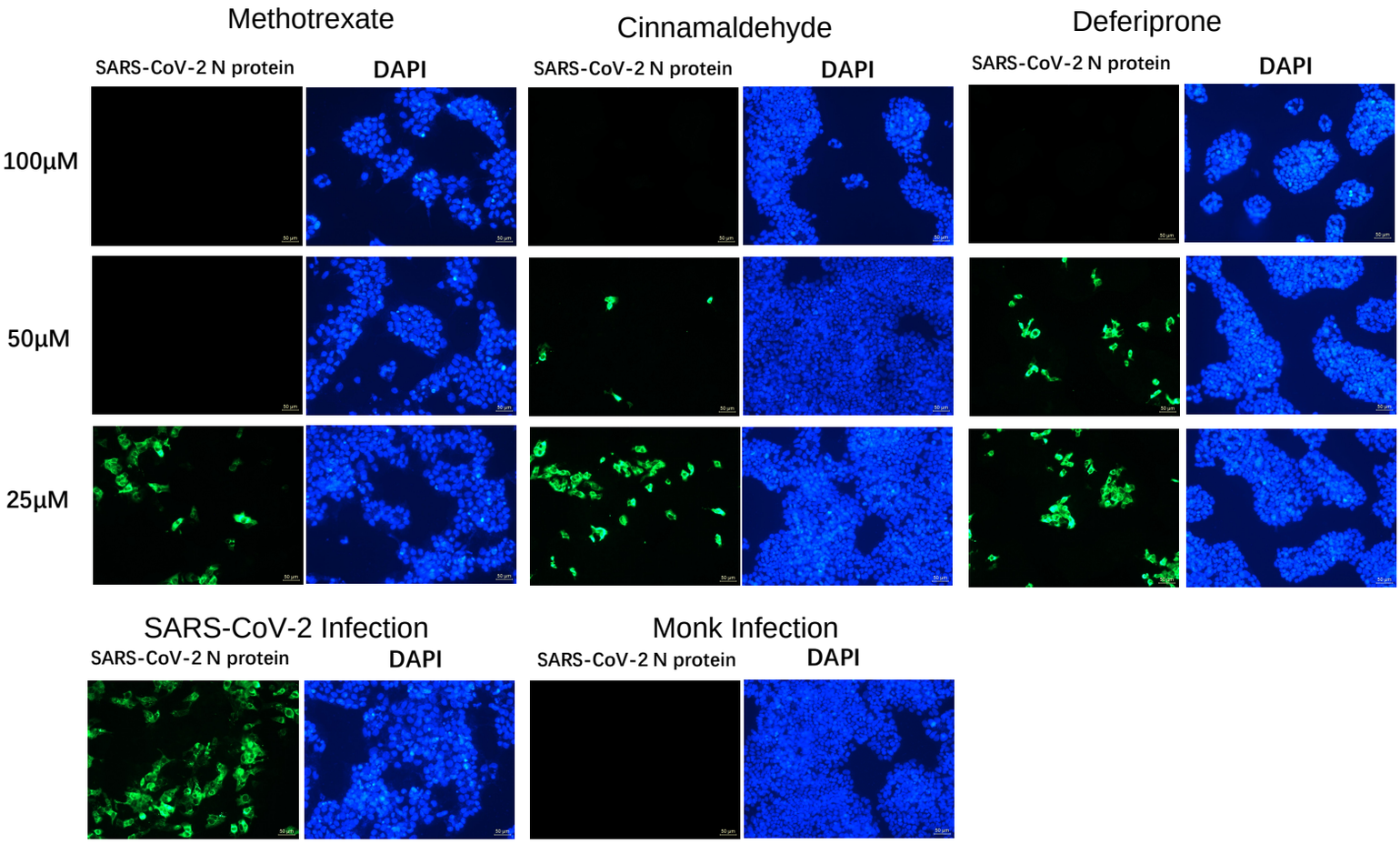

B. Antiviral activity assay of three predicted drugs

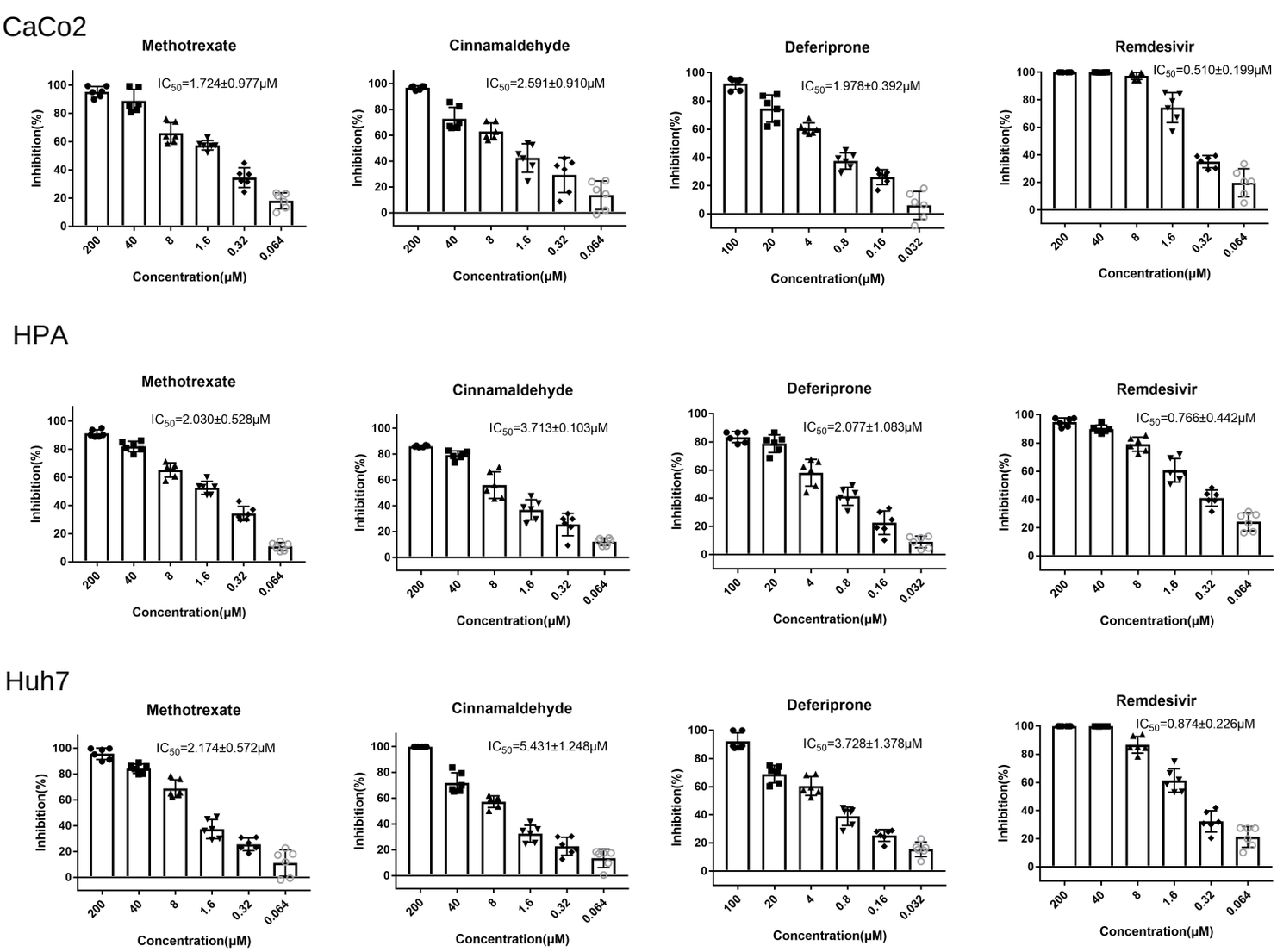

Figure 5

Study	Experimental Events	Experimental Total	Control Events	Control Total	OR	95%−CI	Weight
Hospital−A	25	280	12925	101265	0.67	[0.44; 1.01]	14.6%
Hospital−B	25	540	4725	69420	0.66	[0.44; 0.99]	15.7%
Hospital−C	40	455	7595	58765	0.65	[0.47; 0.90]	24.0%
Hospital−D	35	500	4550	45575	0.68	[0.48; 0.96]	20.7%
Hospital−E	35	685	11480	132980	0.57	[0.41; 0.80]	25.1%
Common effect model		**2460**		**408005**	**0.64**	**[0.55; 0.75]**	**100.0%**
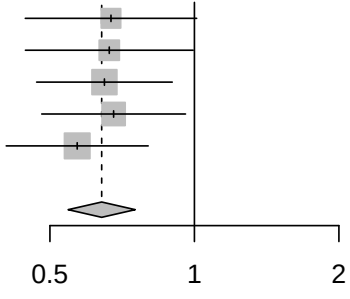
Heterogeneity: $I^2 = 0\%$, $\tau^2 = 0$, $p = 0.96$